Vol.23, No.4, PP.169-177 P-ISSN: 2070-4003 E-ISSN: 2664-5548

Design of HHO Cell for Green Hydrogen Production

Dhuha Ali Moaya¹, Moayad Khalil Ibrahim¹, and Haleemah Jaber Mohammed²

¹Department of Energy Engineering, College of Engineering, University of Baghdad, Baghdad, Iraq ²Department of Medical Physics, College of Science, Uruk University *Corresponding author: doha.ali2309@coeng.uobaghdad.edu.iq

Article Info. **Abstract**

Global warming, driven by scientific and technological progress and rising environmental pollution, has intensified the need for alternative renewable energy sources like hydrogen. This study focused on designing a hydrogenhydrogen oxygen (HHO) cell using primary materials, where stainless steel electrodes (10 cm diameter) were coated with carbon nanotubes (CNTs) via electrochemical deposition. The CNTs were synthesized from potato peel waste, demonstrating an eco-friendly approach to nanomaterial production. Structural and morphological analyses of the CNTs were conducted using scanning electron microscopy (SEM), atomic force microscopy (AFM), and Xray diffraction (XRD), confirming their high surface area and crystalline structure. The research also investigated the impact of electrolyte concentration potassium hydroxide (KOH) on hydrogen production efficiency. By varying electrolyte parameters and applied current, the study monitored gas output per unit time, revealing a significant increase in H2 and O2 flow rates with CNTcoated electrodes. The enhanced performance was attributed to the electrodes' improved conductivity, corrosion resistance, and catalytic activity. These findings highlight the potential of nanotechnology in optimizing renewable energy systems, offering a sustainable solution for green hydrogen production.

Keywords:

HHO cell, Electrochemical Deposition, Hydrogen, Nano- electrode, Concentration.

Article history:

Received Dec. 23, 2024 Revised: May, 03, 2025 Accepted: May, 06,2025 Published:Dec.01,2025

1. Introduction

Gas Global warming is a major issue among many others that the scientific community must find solutions for [1,2]. Effective solutions should aim to reduce pollution in order to preserve the environment for current and future generations. One contemporary possible solution is the use of renewable energy, which is considered a clean and relatively harmless energy source. As a result, numerous research projects and experimental initiatives are being carried out worldwide to promote the use of renewable energy [3,4]. Hydrogen-hydrogen oxygen (HHO) generation cells are presented as a source of green alternative energy due to their ability to combat environmental pollution [5,6]. These cells are environmentally friendly because hydrogen burns completely without producing pollutants or toxic fumes [7,8]. Recently, HHO cell has been developed as an innovative solution for green hydrogen production [9,10]. Additionally, HHO generation cells have also been proposed as a storage for green alternative energy [11,12].

Water electrolysis is the working principle of the HHO generator. Electrolysis has been used to produce hydrogen since the 19th century [13]. Water electrolysis is a promising technique for producing clean water as a sustainable energy source. Current is passed through an electrolyte using an electrode. The flowing current separates water into hydrogen and oxygen gases, which are combined into a mixture called Brown's Gas HHO [14]. The HHO generation cells are of two types according to their construction: the wet cell and the dry cell. The dry cell was adopted in this work. Industrial applications of HHO gas include welding and metal cutting. Currently, it is also used as an additive fuel to conventional fuels to reduce pollutant concentrations emitted during combustion in diesel

and petroleum engine chambers. This process uses water as the main raw material to produce HHO gas without emitting pollutants into the environment [15].

To improve the electrical properties of electrolytic cell electrodes, they are coated with nanomaterial that enhances their physical and mechanical properties. These nanomaterials intersect between the overall structure of the material and the atomic or molecular structure, improving its electrical and mechanical properties. In contrast, the physical properties of the overall material remain constant regardless of its size. However, upon reaching the nanoscale, the properties of the material change according to the size of the nanoparticles and the principle of quantum confinement [16]. Therefore, it is necessary to select promising materials suitable for this work to achieve high quality [17]. Carbon nanotubes are an important and promising material in this regard, and they are prepared using electrochemical deposition techniques [18, 19]. The aim of this study is to design an HHO cell coated with carbon nanotubes through electrochemical deposition and to investigate the electrochemical parameters of the cell.

2. Experiential Work

The cell electrodes were prepared from stainless steel 316L. The stainless steel sheets were of 10 mm thickness and cut into pieces of 5×2 cm² area. These pieces were cleaned in an ultrasonic bath using acetone and ethanol sequentially for 10 minutes. Subsequently, they were immersed in a 20% HF acid solution for ten minutes. Finally, they were rinsed with distilled water.

In this work, carbon nanotubes (CNTs) purchased from (Cheap Tubes Inc-USA, purity 90 wt%, OD: 20-40 nm, ID: 5-10 nm, length: 10-30 nm) was used. The CNTs were oxidized with a mixture of sulfuric acid (H₂SO₄) and nitric acid (HNO₃) at a mixing ratio of 1:3 to introduce a carboxyl group (COOH-), making the tubes more water-dispersible. The CNTs were thoroughly washed with distilled water until the pH reached 7 and dried. An electrolyte was prepared from 10 mg of CNTs in 100 ml of water, and the solution was subjected to a sonication bath for 1 hour. After ensuring the dispersion of the CNTs, the electrochemical process of coating the electrodes with CNTs was then carried out by immersing the electrodes in the prepared electrolyte solution to find the equilibrium between the electrodes and the electrolyte solution [20], as shown in Fig. 1.

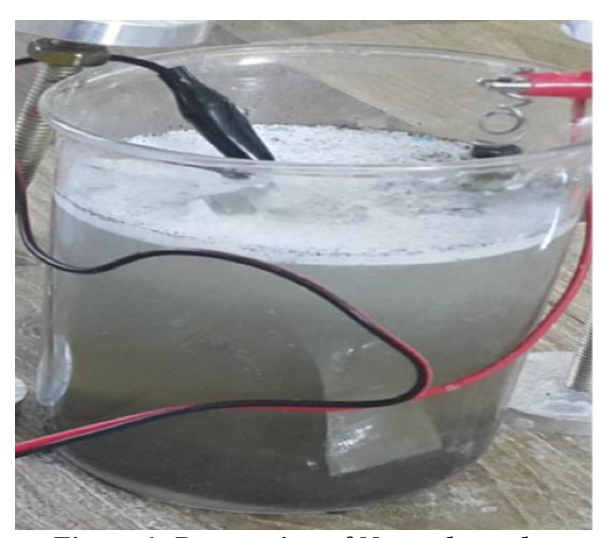


Figure 1: Preparation of Nano electrodes.

2. 1. Preparation of Potassium Hydroxide (KOH) Electrolyte

Potassium Hydroxide (KOH) at 0.0099 M was taken in a 2 L flask containing 500 mL of distilled water. The mixture was exposed to ultrasonic waves for 10 minutes. The flask was then filled with distilled water up to 2 L to prepare a 0.16 M KOH solution. The

flask was subjected to ultrasonic waves for 5 minutes to ensure homogeneity. Two concentrations of KOH solution were prepared, 0.16 M and 0.32 M. Since pure water has low electrical conductivity. Electrolyze solutions such as KOH are added for the increase of ions number, thus improving the electrical conductivity.

2. 2. Design of HHO Cell

Three circular plates of stainless steel 316L with a diameter of 10 cm, one serving as the cathode electrode (the negative terminal), the other as the anode electrode (the positive terminal), and the third as a neutral plate positioned between the two plates to facilitate the electrolysis process. The surfaces of the electrodes were coated with carbon nanotubes, as explained. Two holes, each with a radius of 3 mm, were drilled into all three electrodes to equalize the liquid level and allow the passage of the electrolyte and HHO gas. Circular gaskets with a 10 cm diameter were cut from 1.6 mm thick Ethylene Propylene Diene Monomer (EPDM) rubber, and two transparent acrylic sheets with a diameter of 12 cm were also cut for this design were arranged and fixed until had become a small chamber to hold distilled water mixed with the solution of ammonia hydroxide, as shown in Fig. 2.



Figure 2: The final construction part of dry HHO cell.

3. Results and Discussion

3. 1. X-Ray Diffraction

Fig. 3 shows the X-ray diffraction (XRD) pattern of the CNTs. The CNTs diffraction peaks located at 2θ : 25.5° , 34.5° , and 52.7° are well matched with the Miller indices (hkl) at (110), (002), and (101), respectively, according to the JCPDS Card Number 26-1079 [21]. The crystallite size was determined using the Scherrer equation:

$$D(\mathring{A}) = \frac{K\lambda}{\beta \cos \theta} \tag{1}$$

where D is the crystalline size in nm, λ is the X-ray wavelength (1.54 Å), k is the Scherrer constant equal to 0.89, θ is the diffraction angle, and β is the full width at half maximum (FWHM) in radian.

The results obtained showed that increasing the angle and decreasing the FWHM led to an increase in the crystallite size, as shown in Table 1, which indicates an improvement in the crystallinity of the material. The (002) plane is the main plane and represents the rotation of crystallization, also the planes (100) and (101) showed the arrangement of atoms in the transverse directions. It was noted that the highest crystalline

size was 21 nm at the angle 34.5° of the plane (002). These results agree with those of Duraia et al. [22] and Dore et al. [23].

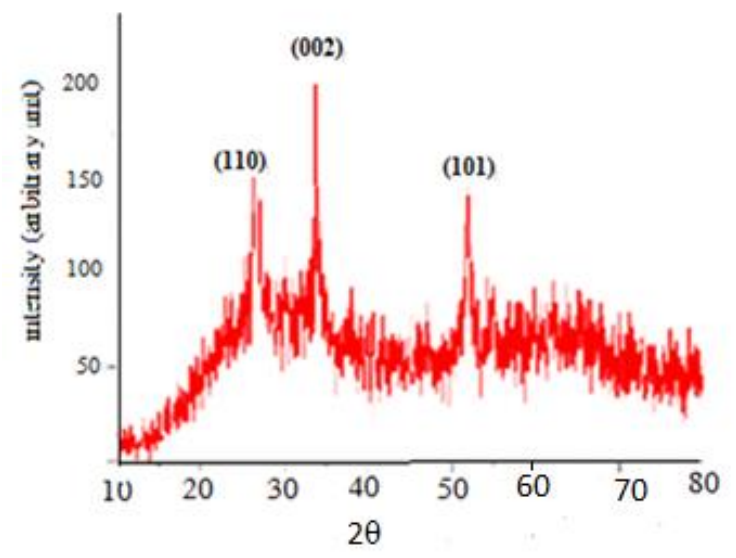


Figure 3: X-ray diffraction of the CNTs.

Table 1: The XRD parameters of CNTs.

Name sample	20	FWHM (degree)	d _{exp.} (nm)	(D) (nm)	Lattice constant hkl	St. cart JCPDS
CNT /SS 316 L	25.5	0.60	0.349	14.0	(110)	26-1079
	34.5	0.40	0.340	21.0	(002)	26-1079
	52.7	0.45	0.20	18.2	(101)	26-1079

3. 2. Scanning Electron Microscopy (SEM) Analysis

Fig. 4 shows the SEM image for the CNTs, it can be noted that the shape and distribution of the grains are different. The grains were spiky in shape, had quasi-uniform distribution, and were vacancy-free. This situation is preferred in the present work because it provides a high surface area by offering more binding sites, thereby enhancing the adsorption activity of reactants and improving the electrical characteristics (potential and current density) required for a high-efficiency cell.

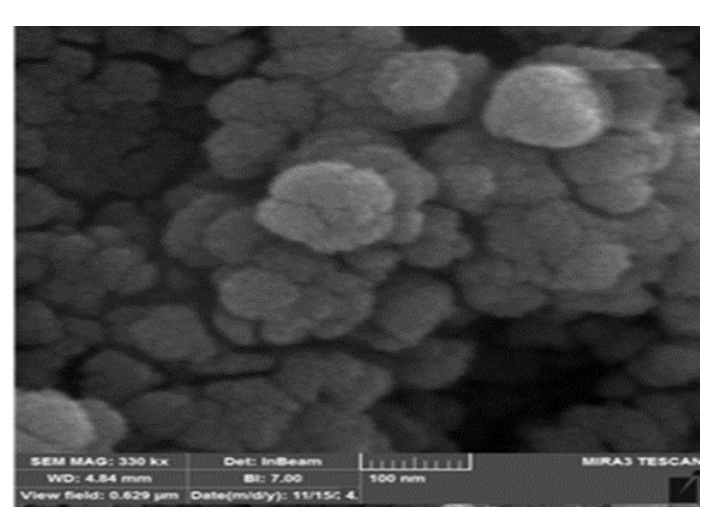


Figure 4: SEM images of the CNTs.

3. 3. Atomic Force Microscopy (AFM) Analysis

The numerous bumps visible in the 3D AFM image of carbon nanotubes indicate that the grain size on the sample surface is larger than the crystalline size shown in XRD and the particle size shown in SEM; this can be attributed to the agglomeration of particles into granules. Also, the increased roughness indicates a high surface area and adsorption activity, which increases the release of hydrogen gas due to the increased conductivity, as shown in Fig. 5 and Table 2.

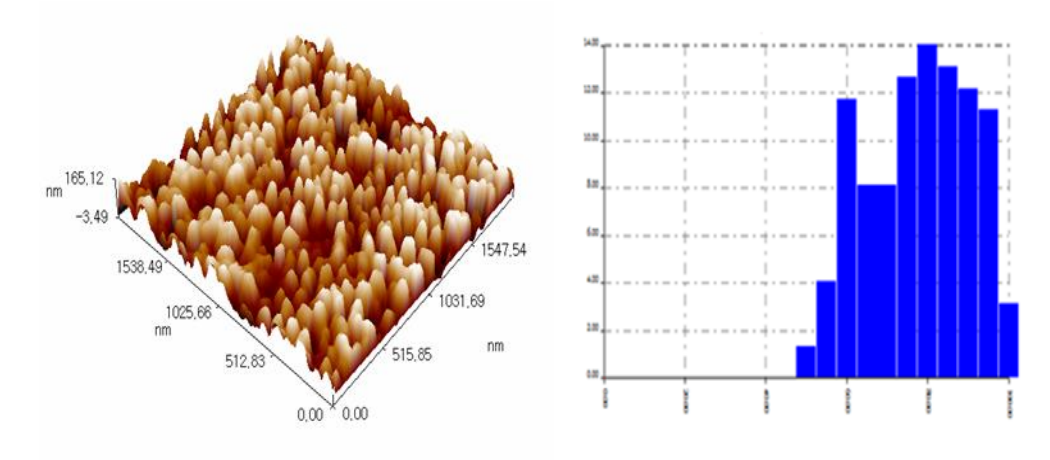


Figure 5: 3-D AFM image of the CNTs.

Table 2: Average roughness and grain size of CNTs.

Thickness of CNTs	Roughness Average	Grain Size	
coating (nm)	(nm)	(nm)	
150	6.32	53.84	

3.4. Test of KOH Concentration

The current passing through the electrolysis cell was studied as a function of KOH concentration. The current was generated at a constant voltage of 12 V; it increased as the KOH electrolyte concentration increased from 0.16 to 0.32 M, as shown in Fig. 6 and Table 3. In Table 3, the first current reading was taken after 10 minutes, then the time was increased to another 5 minutes and a current reading was taken. This process continued until 35 minutes. The results showed the increasing the electrolyte concentration enhances the electron transfer rate between the electrodes as well as the conductivity of the electrodes, ultimately leading to an increase in the electric current generated for all types of electrode surfaces. This, in turn, influenced the rate of water dissociation [24]. However, the increased the KOH concentration reduces the electrical resistance and intensifies the electrical current, thus increased the electrical conductivity and resulting in a decreasing in voltage [25, 26].

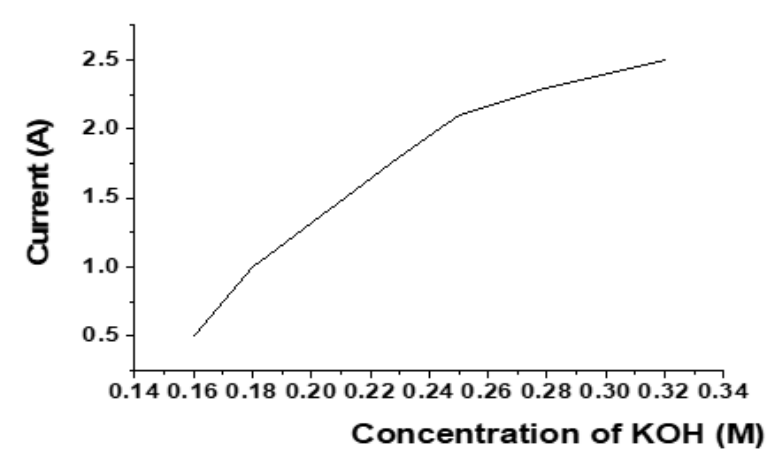


Figure 6: Relationship between the current and Concentration of KOH.

Table 3: Relationship between electrochemical parameters and time.

Tubic 5. Retutionship between electrochemical parameters and time.					
Time (min)	Current (A)	Voltage (V)	Concentration of KOH (M)	H ₂ Volume (ml)	
10	0.5	12	0.16	0	
15	1	12	0.18	1.3	
20	1.8	12	0.23	4.2	
25	2.1	12	0.25	8.4	
30	2.3	12	0.28	12.5	
35	2.5	12	0.32	18.6	

3.5. HHO Cell Results

Hydrogen was produced at the cathode made of 316 stainless steel coated with carbon nanotubes. The results showed that KOH solution significantly activated the anode, thus allowing negative hydroxide ions to pass through it [27]. Also, electrical conductivity increased with time, so did the flow rate of hydrogen and oxygen gases, as shown in Fig. 7. Coating the cell electrodes with CNTs enhanced the electrocatalytic activity, thus increasing its efficiency for hydrogen production. These results agree with the results of Ahmassri et al. [28].

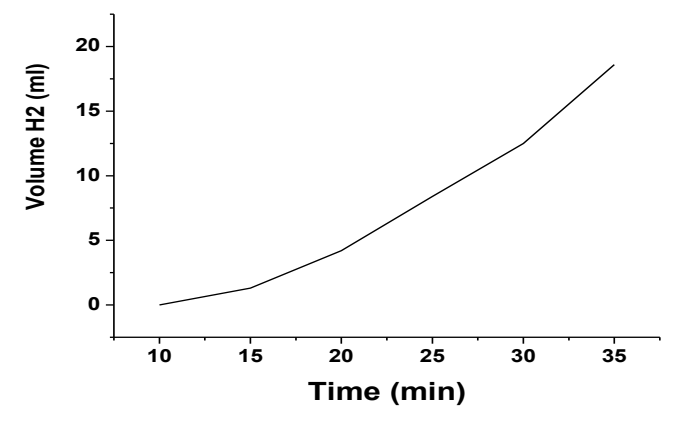


Figure 7: Relationship between the volume of the produced hydrogen gas with time.

3.6. Hydrogen Gas Flow Rate Measurements

The hydrogen gas flow rate was measured when using the CNTs-coated electrodes and when using uncoated electrodes; all other conditions were kept the same, as clarified in Table 4. Hydrogen gas flow rate nearly doubled with the use of the coated electrodes. Coating the electrodes with CNTs helped improve their electrical conductivity and high stability, thus increasing and improving hydrogen production [29,30]. By investigating the relationships between these variables and the underlying reaction mechanisms, deeper insights can be gained into the science of electrolysis and develop strategies to improve the performance and efficiency of the HHO generator [31,32]. The cell generator can produce more gas depending on the cell type of the electrode [33, 34].

and coated nanoelectrodes.					
CNTs-coated electrodes	CNTs-uncoated electrodes	Conditions			
10 V	10 V	Input voltage			
1.5 A	1.5 A	Input current			
183.75 cm ²	183.75 cm ²	The active area of the cell			
0.28 M	0.28 M	Concentration of electrolyte solution			
30 s	30 s	Time used to measure the gas flow rate			

Flow rate of hydrogen gas

45 ml/min

Table 4: The operation condition for measurement of the hydrogen gas flow rate for uncoated and coated nanoelectrodes.

4. Conclusions

80 ml/min

In this work, an HHO cell was fabricated using 316 L stainless steel electrodes coated with CNTs and an electrolyte solution of KOH to produce hydrogen. The XRD results showed that the coating of CNTs was crystalline, with the rotation peak at (002). The SEM image showed spiky-shaped grains with a quasi-uniform distribution and vacancy-free. The AFM images indicated a high roughness value, resulting in a high surface area and adsorption activity. In the OHH cell, the generated current at a constant voltage increased with the electrolyte concentration of KOH. The OHH cell electrical conductivity increased with increasing time. The CNTs coated cell electrodes enhanced the electrical conductivity and their stability, and improved hydrogen production.

Acknowledgment

I would like to express my sincere thanks and deep gratitude to everyone who contributed to the completion of this research, especially Dr. Haleemah, for his continuous support and guidance, which had a significant impact on enriching the content of this work. I would also like to thank the Al-Razi Laboratory in Al-Mansour, Baghdad, for their cooperation in completing the research tests.

Conflicts of Interest

The authors declare they have no competing interests.

References

 M. Haider, S. Hussain, H. Farid, U. Shahid, A. Ahmed, and N. Abbas, Pakistan Journal of Engineering and Technology, PakJET Multidisciplinary & Peer Reviewed, 4, 73, (2021). https://doi.org/10.51846/pakjet.v4i2.

- 2. S. Pamford, K. Essuman, A. Nyamful, V. Y. Agbodemegbe, and S. K. Debrah, International Journal of Engineering Science Invention (IJESI), 8, 01, May, (2019).
- 3. K. C. Divya and J. Østergaard, Electric Power Systems Research, Elsevier, **79**(4), 511, (2009). https://doi.org/10.1016/j.epsr.2008.09.017.
- X. Zheng, S. Zhang, X. Zheng, Z. Zhuang, M. Gao, Y. Liu, and W. Sun, Adva. Mate, 37, 2502127, (2025). https://doi.org/10.1002/adma.202502127.
- 5. C. Akl, J. Dgheim, and N. El Hajj, Sustainability, 17, 3811, (2025). https://doi.org/10.3390/su17093811.
- 6. A. A. Ingle, International Research Journal of Engineering and Technology (IRJET), 8, 489 (2021).
- 7. H. Enshasy, Q. Abu Al-Haija, H. Al-Amri, M. Al-Nashri, and S. Al-Muhaisen, Acta Electronica Malaysia (AEM), 3, 09, (2019). http://doi.org/10.26480/aem.02.2019.09.15.
- 8. Z. Su, P. Ding, W. Su, X. Li, Y. Li, and Y. Wang, Frontiers in Endocrinology, **15**, 1386021, (2024). https://doi.org/10.3389/fendo.2024.1386021.
- 9. A. Z. Abdulameer, Z. Buntat, R. Naveed Arshad, and Z. Nawawi, International Journal of Recent Technology and Engineering (IJRTE), **8**, 490, July, (2019).
- 10.H. M. Enshasy, Q. Abu Al-Haija, H. Al-Amri, M. Al-Nashri, S. Al-Muhaisen, and M. Al-Tarayrah, WSEAS Transactions on Systems, (2020). https://doi.org/10.37394/23202.2020.19.35.
- 11. H. J. Mohammed and N. A. Ali, Univ. Thi-Qar J. Sci. **7**, 106 (2020) https://doi.org/10.32792/utq/utjsci/v11i2.
- 12. B. Sharma, S. Manna, V. Saxena, P. Raghuvanshi, M. Alsharif, and M. Kim, Scien. Reports, **15**, 661, (2025). https://doi.org/10.1038/s41598-024-84296-1.
- 13. M. Streblau, B. Aprahamian, M. Simov, and T. Dimova, in 18th International Symposium on Electrical Apparatus & Technologies, 1, (2014). http://doi.org/10.1109/SIELA.2014.6871898.
- 14. N. Afgan and A. Veziroglu, Sustainable resilience of hydrogen energy system, International Journal of Hydrogen Energy, **37**, 5461, (2012). http://doi.org/10.1016/j.ijhydene.2011.04.201.
- 15. J. Barton and R. Gammon, Journal of Power Sources, **195**, 8222, (2010) http://doi.org/10.1016/j.jpowsour.2009.12.100.
- W. Lee, B. Hawkin, D. M. Day, and D. C. Reicosky, Energy & Environmental Science, 3, 1695, (2010).
 DOI: https://doi.org/10.1039/C004561F.
- 17. V. Mohanraj and Y. Chen, Tropical Journal of Pharmaceutical Research, 5, 561, (2006). https://doi.org/10.4314/tjpr.v5i1.14634.
- 18. O. S. Nille, A. S. Patil, R. D. Waghmare, V. M. Naik, D. B. Gunjal, G. B. Kolekar, and A. H. Gore, Valorization of Agri-Food Wastes and By-Products, Chapter 11, 219 (2021). https://doi.org/10.1016/B978-0-12-824044-1.00046-5.
- 19. V. Sharma, S. Kumar, I. Kainthla, M. Shandilya, and S. Thakur, Waste Derived Carbon Nanomaterials **2**, 103, (2025). https://doi.org/10.1021/bk-2025-1495.ch006.
- 20. Y. Yu, L. Li, E. Liu, X. Han, J. Wang, Y. Xie, and C. Lu, Carbon, **187**, 97, (2022). https://doi.org/10.1016/j.carbon.2021.10.071.
- 21. M. Hossain, A. Roy, M. Molah, and M. Uddin, Springer Plus **3**(1) 134, (2014). https://doi.org/10.1186/2193-1801-3-73.
- 22. E. Duraia, M. Opoku, and G. Beall, Scientific Reports, **14**(1), 16405, (2024). https://doi.org/10.1038/s41598-024-65893-6.
- 23. J. Dore, A. Burian, and S. Tomtta, Acta Physica Polonica, **98**(5), 457 (2000). https://doi.org/10.12693/APhysPolA.98.457.
- 24. I. Dincer, and M. Agelin-Chaab, J. of Power Sour. **632**, 236326, (2025). https://doi.org/10.1016/j.jpowsour.2025.236326.
- 25. A. Ursua, L. M. Gandia, and P. Sanchis, Proceedings of the IEEE, **100**, 410, (2011). https://doi.org/10.1109/JPROC.2011.2156750.
- 26. K. Zeng and D. Zhang, Progress in Energy and Combustion Science, **36**, 307, (2010). https://doi.org/10.1016/j.pecs.2009.11.002.
- 27. M. Allah, A. Hariri, and K. Mohamed, J. of Adva. Rese. in Fluid Mech. and Ther. Scie., **101**, 45 (2022). https://doi.org/10.37934/arfmts.101.1.4558.
- 28. X. Bi, G. Wang, D. Cui, X. Qu, S. Shi, D. Yu, and Y. Ji, Fuel, **380**, 133209. (2025). https://doi.org/10.1016/j.fuel.2024.133209.
- 29. A. D. Franklin, M. C. Hersam, and H.-S. P. Wong, Science, **378**, 726, (2022). https://doi.org/10.1126/science.abp8278.
- 30. K. Rani, G. Singh, S. Narwal, B. Chopra, and A. Dhingra, Current Nanomedicine, **15**, 50, (2025). https://doi.org/10.2174/0124681873294822240517073406.
- 31. Z. K. Abdulrahman, A. H. Al-Mamoori, and T. Y. Al-Doori, Int. J. Hydrogen Energy, **48**, 27891 (2023). https://doi.org/10.1016/j.ijhydene.2023.06.112.
- 32. N. A. Ali, B. T. Chied, and H. J. Mohammed, in *Proceedings of the Fourth Conference for Low Dimensional Materials and its Applications* (Iraqi Journal of Science, Special Issue, 2018).
- 33. H. J. Mohammed, N. A. Ali, and B. H. Jwad, IOP Publishing, Journal of Physics: Conference Series, **1660**, 012046 (2020). http://doi.org/10.1088/1742-6596/1660/1/012046.

34. H. J. Mohammed and N. A. Ali, AIP Conference Proceedings, **2144**, 030002, (2019). https://doi.org/10.1063/1.5123072.

تصميم خلية HHO لأنتاج الهيدروجين الأخضر

ضحى على مؤيد¹ ومؤيد خليل أبراهيم¹ وحليمة جابر محمد² أقسم هندسة الطاقة، كلية الهندسة، جامعة بغداد، بغداد، العراق تُسم الفيز باء الطبية، كلية العلوم، جامعة او روك

الخلاصة

أدى الاحتباس الحراري، المدفوع بالتقدم العلمي والتكنولوجي وتزايد التلوث البيئي، إلى تزايد الحاجة إلى مصادر طاقة متجددة بديلة مثل الهيدروجين. ركزت هذه الدراسة على تصميم خلية هيدروجين-اكسجين (HHO)باستخدام مواد أولية، حيث طُلِيت أقطاب من الفولاذ المقاوم الصدأ (قطرها 10 سم) بأنابيب الكربون النانوية (CNTs)عبر الترسيب الكهروكيميائي. صنعت هذه الأنابيب من مخلفات قشور البطاطس، للصدأ وقط مما يُظهر نهجًا صديقًا للبيئة لإنتاج المواد النانوية. أُجريت تحاليل هيكلية ومور فولوجية لهذه الأنابيب باستخدام المجهر الإلكتروني الماسح (SEM)، ومبهر القوة الذرية (AFM)، وحيود الأشعة السينية (XRD)، مما أكد ارتفاع مساحة سطحها وبنيتها البلورية. كما بحث البحث في تأثير تركيز الإلكتروليت والتيار المطبق، رصدت الدراسة في تأثير تركيز الإلكتروليت والتيار المطبق، رصدت الدراسة إنتاج الغاز لكل وحدة زمنية، وكشفت عن زيادة كبيرة في معدلات تدفق H2 وO2 مع الأقطاب المغلفة بأنابيب الكربون النانوية. يُعزى الأداء المُحسن إلى تحسين توصيل الأقطاب الكهربائية ومقاومتها التأكل ونشاطها التحفيزي. تُسلِّط هذه النتائج الضوء على إمكانات تقنية النانو في تحسين أنظمة الطاقة المتجددة، مُقدِّمةً حلاً مستدامًا لإنتاج الهيدروجين الأخضر.

الكلمات المفتاحية: خلية HHO، الترسيب الكهروكيميائي، الهيدروجين، القطب النانوي، التركيز.